# Correlation of the Detachment of Two-Dimensional Turbulent Boundary Layers

S. J. Kline,* J. G. Bardina,† and R. C. Strawn‡
*Stanford University, Stanford, California*

**An improved single-variable correlation is developed for incipient and full detachment, and for reattachment of turbulent boundary layers on two-dimensional surfaces. The correlation is shown to agree with 1) the wall-wake law of Coles; 2) the criterion for detachment of Sandborn and Kline; 3) a large amount of old flow-visualization data; and 4) new measurements of time-averaged fraction of forward flow. Relationships among the correlation, the underlying physics, and the implications for computations are discussed. The results clarify long-standing confusion between incipient and full detachment of turbulent boundary layers with regard to both correlation and computation.**

## Nomenclature

$A_{\text{eff}}$ = effective two-dimensional channel area $=(W-\delta_L^*-\delta_u^*)$
$C$ = constant in Coles velocity profile = 5.0
$\bar{C}_f$ = friction coefficient $=2\bar{\tau}_w/\rho U_\infty^2 = 2K^2 V_T |V_T|$
$H$ = shape factor $=\delta^*/\theta$
$h$ = shape factor $=(H-1)/H=(\delta^*-\theta)/\delta^*$
$K$ = von Kármán constant = 0.41
$R$ = equilibrium velocity profile constant
$Re_{\delta^*}$ = displacement thickness Reynolds number $=(\delta^* U_\infty)/\nu$
$S$ = component of distance along the wall
$U$ = velocity component parallel to the wall in the boundary layer
$U_\infty$ = boundary-layer edge velocity
$u_\tau$ = shear velocity $(\text{sign}\ \tau_w)\sqrt{|\bar{\tau}_w|/\rho}$
$V_B$ = dimensionless wake amplitude $=2u_\tau \Pi(x)/U_\infty K$
$V_T$ = nondimensional shear velocity $=u_\tau/KU_\infty$
$W$ = passage width for two-dimensional internal flow
$y$ = component of distance normal to wall
$\gamma_p$ = fraction of forward flow in the viscous sublayer
$\delta$ = boundary-layer thickness
$\delta^*$ = boundary-layer displacement thickness
$\theta$ = boundary-layer momentum thickness
$\Lambda$ = boundary-layer shape factor $=\delta^*/\delta$
$\nu$ = fluid kinematic viscosity
$\Pi(x)$ = wake parameter in Coles velocity profile
$\rho$ = fluid density
$\tau_w$ = wall shear stress

*Superscript*
$(\bar{\ })$ = time-averaged quantity

## Introduction

THE objectives of this paper are twofold: 1) to provide an improved correlation for two-dimensional flow detachment of turbulent boundary layers, using appropriate boundary-layer integral parameters, and 2) to provide the basis for a design method which allows for the preselection of "stall margin" in turbulent boundary layers. The term stall margin is used here to denote a measure of the proximity of a boundary layer to detachment in an appropriate metric.

This paper emphasizes that the physics of the detachment process in the turbulent case is fundamentally different from that of the laminar case. The paper first describes the physics in terms of recent measurements, and then relates these physical pictures to improved correlations and to implications for modeling and computation.

A remark concerning terminology is appropriate here. We use the word detachment to represent the process (or location) where a boundary layer (or limiting streamline) moves away from a solid surface. The term separation represents the flow phenomenon or region that includes detachment, a reverse flow zone, and possibly a reattachment zone.

## Definition of Separation States: Flow Physics

Sandborn and Kline[1] emphasized that two-dimensional turbulent flow detachment from a faired surface is not a single event, but is rather a process, a transition from attached to detached flow. Turbulent detachment with steady time-mean flow occurs over a zone, not along a single line normal to the flow, as in the laminar case. Moreover, they noted that the turbulent detachment process involves increasing amounts of backflow (averaged over time) as one moves through the detachment zone. This flow model has been independently verified by Simpson et al.[2]

One way to quantify the spectrum of separating states is to introduce the parameter $\gamma_p$, the fraction of instantaneous forward flow in the viscous sublayer. Using this parameter, one can present a picture of turbulent detachment, as shown in Fig. 1. Curve LD on Fig. 1a pictures the accepted model for a steady, two-dimensional, laminar boundary layer. Note that this laminar model implies that the flow is forward 100% of the time up to the location of a detachment line where $C_f=\bar{C}_f=0$. At this location, a sudden shift occurs to 0% forward flow (100% backflow). Thus a trace of time-averaged fraction of forward flow, $\gamma_p$ vs $x$ for a detaching laminar boundary layer is essentially a step function. It is doubtful if this step function is ever completely realized for separating flow, since most separating flows are at least somewhat unsteady. Nevertheless, the model is a helpful one for laminar boundary layers.

Unfortunately, at least from the viewpoint of simplicity, turbulent detachment on a faired surface does not follow the laminar model of curve LD in Fig. 1a. The detachment process for a two-dimensional turbulent boundary layer is a

Presented as Paper 81-1220 at the AIAA 14th Fluid and Plasma Dynamics Conference, Palo Alto, Calif., June 23-25, 1981; submitted July 13, 1981; revision received March 25, 1982. 

*Professor, Mechanical Engineering Department.
†Formerly Research Assistant, Mechanical Engineering Department.
‡Research Assistant, Mechanical Engineering Department. Student Member AIAA.

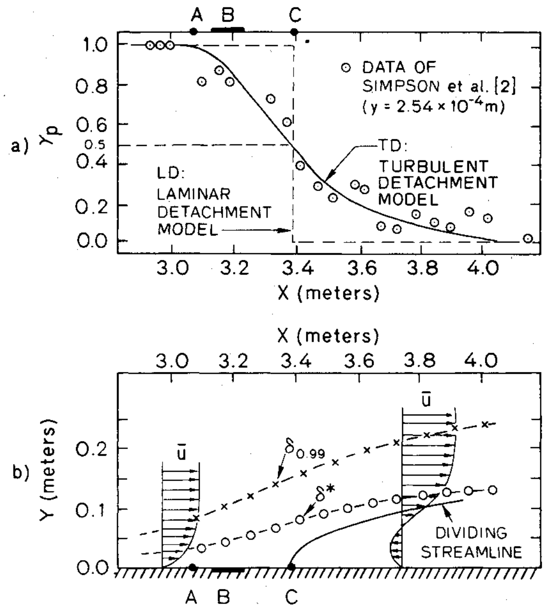


**Fig. 1 Schematic of two-dimensional detachment.**

gradual one on faired surfaces; it covers a zone that may be long or short, but is of finite length in the streamwise direction. Note that the curve TD of Fig. 1a is not hypothesized; it is drawn from the data of Simpson et al.[2] Additional measurements recently have been reported by Ashjaee et al.[4] Their data show the same type of behavior. These two sets of data are by far the most detailed and accurate currently available; moreover, the two data sets are the result of entirely different experimental methods. Simpson et al.[2] used a laser anemometer, and Ashjaee et al.[4] used a three-wire thermal tuft in the wall layers, as described by Eaton et al.[5]

The essence of the difference between the laminar and turbulent detachment cases is the unsteadiness of the flow. In the turbulent case, small bits of backflow appear and disappear near the wall as a function of time at a given location. This is recorded clearly by the data establishing the TD curve in Fig. 1a and independently by Ashjaee et al.[4] using different instruments. The entire line of detachment does not move up- and downstream as a unit in turbulent separation. Rather, small three-dimensional elements of flow move upstream for a distance, are "mixed out" by Reynolds stresses, and then once again carried downstream. These motions are clearly visible in the visual studies of Schraub and Kline.[6] They appear to involve reverse flows of low-speed streaks originating in the viscous sublayer. These reverse flows occur in regions of low kinetic energy and are caused by forces arising from the adverse pressure gradient, but the details have not been well studied. Moreover, such backflows of the low-speed streaks in a laboratory frame of reference are *not* observed for zero or favorable pressure gradients in the visual studies of Schraub and Kline[6] or of Kline et al.[7]

Another key point regarding turbulent detachment is that zero wall shear is created by an average over three-dimensional, time-dependent, backward, forward, and up and down motions. In the laminar, truly steady case, zero wall shear is created by an absence of motion.

The same remarks concerning zero wall shear apply qualitatively to reattachment, but the motions at reattachment are even stronger in the turbulent case, owing to the larger fluctuations in free shear layers. This accounts for the very high, measured values of heat transfer (Stanton number) at turbulent reattachment (where $\bar{C}_f = 0$). The heat transfer data for reattachment thus also strongly support the model under discussion. Some further details are given by Eaton and Johnston.[8]

Given the physical processes described, the parameter $\gamma_p$ can be taken as a metric for what we might call "degree of detachment." Three somewhat arbitrary stations in this metric are shown in Fig. 1b. At A, one first observes measurable backflows near the wall, that is, $\gamma_p = 0.99$. In zone B, appreciable backflow occurs $(0.80 < \gamma_p < 0.95)$, and we denote this zone as "incipient detachment." The zone of incipient detachment is important since the displacement thickness of the boundary layer begins to increase rapidly here, thus creating difficulties in numerical computation for conventional boundary-layer schemes. Finally, we denote point C as the location of full detachment where $\bar{C}_f = 0$ and $\gamma_p \cong 0.50$. The symbol $\cong$ is used for $\gamma_p$ rather than the exact equality, because an identity of location requires symmetry of the histogram of velocity fluctuations. The data of Eaton and Johnston[5] indicate this condition is fulfilled to within the uncertainty of their measurements. For practical purposes, it appears that $\bar{C}_f = 0$ and $\gamma_p = 0.50$ coincide in $x$ location. However, only a few cases have been measured thus far.

A remark regarding instrumentation is also important. The results of cylindrical or other single element hot-wire or hot-film anemometers at or near turbulent detachment or reattachment are distinctly misleading, since both instruments record fluctuations without regard to direction and thus rectify fluctuations when the flow direction reverses. Thus, conventional probes can not indicate when $\bar{C}_f = 0$ in turbulent detachment or reattachment. Visualization techniques for determining the location of detachment or reattachment (oil streaks, talcum dust, wool tufts, etc.) also suffer difficulties. In particular, they lack a quantitative interpretation that can be related to the detachment picture of Fig. 1. It is unlikely that different types of visualization techniques would respond to local three-dimensional transient backflows in the same manner. Hence, we must expect that detachment location determined by visual studies using different techniques will correspond to various values of $\gamma_p$. We shall see this is the case in the results that follow.

Given these remarks on the physics and the expected response of instrumentation to the difficult measurement conditions, we have set a basis for seeking an improved correlation for turbulent boundary-layer detachment.

## Previous Correlations for Separation

Many early correlations for detachment centered on examining the boundary-layer shape factor. For example, Cebeci and Bradshaw[9] present constant $H$ criteria for separation where $H_{sep}$ ranges from 1.8 to 2.4. These constant $H$ criteria were intended to represent the position of full boundary-layer detachment (i.e., $\bar{C}_f = 0$).

Sandborn and Kline[1] used a two-parameter model as a criterion for incipient separation. Their work correlated a number of experimentally determined incipient separation points in the plane of $H$ vs $\Lambda$, and arrived at the following criterion for incipient separation.

$$H_{sep} = 1 + [1/(1 - \Lambda_{sep})] \quad (1)$$

Equation (1) seems to correlate all available data for incipient separation, as will be shown later in this paper.

Senoo and Nishi[10] also used a two-parameter detachment criterion. They present a correlation for incipient detachment in diffuser flow given by Eq. (2).

$$H_{sep} = 1.8 + 7.5(\delta^*/W)_{sep} \quad (2)$$

In Eq. (2), $(\delta^*/W)_{sep}$ is a measure of the boundary-layer blockage at separation. Later in this paper, we shall discuss Eq. (2) as it relates to the present work.

## Velocity Profile Family for Detaching and Reattaching Flows

A generally accepted form for mean velocity profiles in equilibrium two-dimensional turbulent boundary layers is a log "law" of the wall matched to a correlation for the wake region, as given by Coles.[11] Coles' combined "wall-wake" formulation can be written as

$$\frac{\bar{U}}{u_\tau} = \frac{1}{K}\ell n\left(\frac{yu_\tau}{\nu}\right) + C + \frac{\Pi(x)}{K}\left(1-\cos\frac{\pi y}{\delta}\right) \tag{3}$$

This velocity profile family has shown remarkable success in correlating a wide range of attached turbulent boundary-layer flows. Experience shows that this correlation is remarkably tenacious under many forms of perturbation, as indicated, for example, by Coles and Hirst[12] and a great number of other studies. Equation (3) appears to correlate the vast majority of turbulent boundary layers. It seems to become inadequate only for relatively rare cases that are quite far from an equilibrium between the inner and outer zones of the boundary layer. For detached flows, however, Eq. (3) as originally formulated encounters difficulty, since $u_\tau$ becomes negative and the log term is then undefined. In order to remedy this problem, Kuhn and Nielsen[14] and later Ghose and Kline[13] presented a modified definition of $u_\tau$ as

$$u_\tau = (\text{sign}\bar{\tau}_w)\sqrt{|\bar{\tau}_w|/\rho} \tag{4}$$

With this new definition, Eq. (3) can be cast in the form

$$\frac{\bar{U}}{U_\infty} = 1 + V_T \ell n\frac{y}{\delta} - V_B\cos^2\frac{\pi y}{2\delta} \tag{5}$$

where $V_B$ is a redefined wake amplitude, $V_B = 2u_\tau\Pi(x)/KU_\infty$; and $V_T$ is a dimensionless shear velocity, $V_T = u_\tau/KU_\infty$.

Equation (5) is identical to Eq. (3) for attached flows, but can represent detached flows as well. The ability of Eq. (5) to represent a detached flow is demonstrated in Fig. 2. Further evidence is also given by Bardina et al.[15] and Ghose and Kline.[13]

Equation (5) does not correlate adequately some flows that have very strong wall curvature, boundary-layer suction, or blowing, or strong normal body forces as found in rotating systems. The detachment correlation proposed in what follows uses the velocity profiles of Eq. (5) as essential input. Hence, it will be limited to the class of flows represented by Eq. (5).

## Improved Correlation for Detachment

Using the appropriate definitions for boundary-layer displacement and momentum thickness, the modified Coles' velocity correlation of Eq. (5) can be integrated directly to yield the equations

$$h/\Lambda = 1.5 + 0.179(V_T/\Lambda) + 0.321(V_T/\Lambda)^2 \tag{6}$$

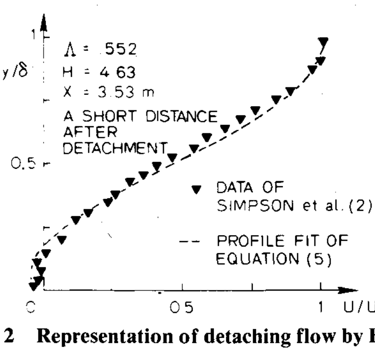


Fig. 2 Representation of detaching flow by Eq. (5).

where $V_T$ is given implicitly by

$$V_T = \frac{1-2\Lambda}{\ell n(|V_T|/\Lambda) + \ell n(KRe_{\delta^*}) + 0.05} \tag{7}$$

Here, $h$ and $\Lambda$ are shape factors defined as

$$h = \frac{\delta^* - \theta}{\delta^*}, \qquad \Lambda = \frac{\delta^*}{\delta} \tag{8}$$

Thus, for boundary layers that can be correlated by the modified Coles' wall-wake profile, Eq. (5), there is a unique relation between the two shape factors $\Lambda$ and $h$ given by Eqs. (6) and (7).

Equations (6) and (7) are compared with data from eight attached, detaching, and reattaching flows in Fig. 3. These flows are chosen to represent the most accurate known data for a wide variety of cases. Figure 3 shows that Eqs. (6) and (7) are remarkably successful in correlating this very wide range of data.

Similar shape factor relations can be obtained by using different velocity profile representations. Sandborn[19] showed that the Clauser requirements for a true equilibrium boundary layer can be written as

$$h = R\Lambda \tag{9}$$

Here $R$ is a constant which defines a particular family of equilibrium profiles. Equation (9) is identical to the high Reynolds number result of Eqs. (6) and (7) when $R = 1.5$. The flat-plate value of $R = 9/5$ agrees well with Eqs. (6) and (7) for low values of $\Lambda$.

A simple power law profile $u/U_\infty = (y/\delta)^n$ can be integrated to give

$$h = 2\Lambda/(1+\Lambda) \tag{10}$$

This result agrees well with the correlation of Eqs. (6) and (7) up to a value of $\Lambda = 0.4$. A third shape factor relation is presented in Fig. 3 and is obtained from Head's entrainment

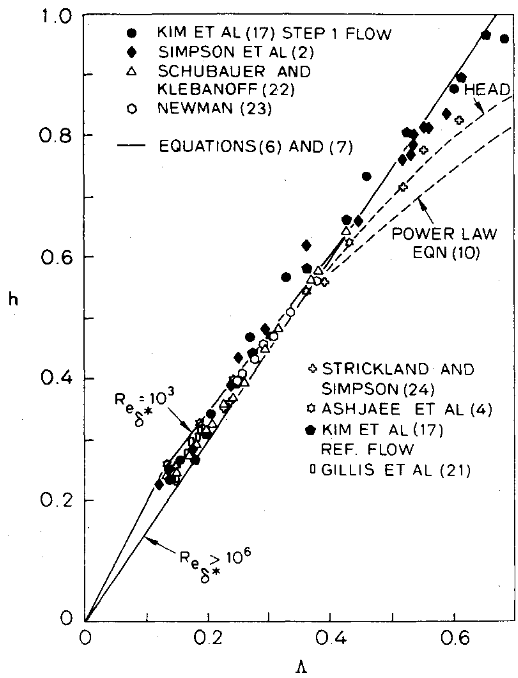


Fig. 3 Detachment and reattachment in the $h$-$\Lambda$ plane.

correlation as described in Ref. 9. All of these results show a good agreement with the correlation of Eqs. (6) and (7).

Since data from actual experiments are presented in Fig. 3, it was necessary to calculate $\Lambda = \delta^*/\delta$ in terms of $\delta_{995}$ for the experimental data points. In general, the value of $\delta$ defined in terms of Eqs. (6) and (7) can be shown to agree with experimentally measured values of $\delta_{995}$. A sampling of 83 velocity profiles from data given by Coles and Hirst[12] has been examined to reveal a mean discrepancy of 1.8%, with a standard deviation 7.6%, between interpolated values of $\delta_{995}$ and those values of $\delta$ calculated by Coles in a manner consistent with Eqs. (6) and (7). Thus, it is expected that values of $\delta$ defined by Eqs. (6) and (7) should correspond approximately to measured values of $\delta_{995}$.

## Properties of the $h$-$\Lambda$ Plane

Studying detachment and reattachment in the $h$ vs $\Lambda$ plane has the following two important advantages.

1) The parameters $h$ and $\Lambda$ are both nondimensional and have the range 0-1 (unlike $H$, which varies from 1 to infinity, and $\theta$, $\delta^*$, and $\delta$, which are dimensional).

2) The relation between $h$ and $\Lambda$ given by Eqs. (6) and (7) is approximately linear and only weakly dependent on $Re_{\delta^*}$ for low values of $\Lambda$. The relation becomes linear and independent of $Re_{\delta^*}$ for $\Lambda > 0.30$ (since $V_T$ becomes small). This property allows simple integration through detachment or reattachment.

By examining the $h$-$\Lambda$ correlation of Eqs. (6) and (7), one can reach a number of useful conclusions and generalizations concerning turbulent boundary-layer detachment. First of all, the skin friction parameter $V_T$ in Eq. (7) takes on negative values for $\Lambda > 0.5$ and positive values for $\Lambda < 0.5$. When $\Lambda = 0.5$, the skin friction is zero. Thus, one condition which arises out of the modified Coles velocity profile is that full boundary-layer detachment ($\bar{C}_f = 0$) occurs when $\Lambda = 0.5$. This result was first presented by Coles[11] in his original paper. At $\bar{C}_f = 0$, the $\Lambda$-$h$ correlation also yields $h = 0.75$ and $H = 4.0$; these values of $h$ and $H$ follow from Eqs. (6) and (7) without any further assumptions.

The intersection of the Sandborn-Kline criterion for incipient detachment with the $h$-$\Lambda$ relation for the Coles wall-wake formulation should delineate incipient detachment for all cases that are near equilibrium. This intersection lies at $\Lambda = 0.42$, $h = 0.63$, and $H = 2.70$. Figure 4 presents data for

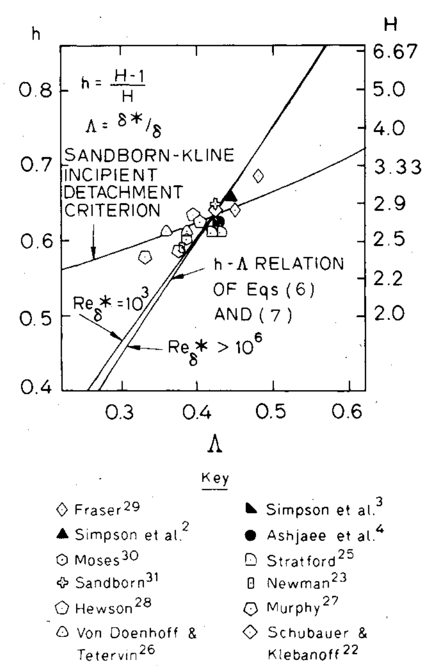


**Fig. 4 Experimental data for location of (incipient) detachment in $h$-$\Lambda$ coordinates.**

detachment locations taken from 17 different experiments. These are all the suitable data found in the literature that comply with the restrictions of Eq. (3); two-dimensional, incompressible flow on faired surfaces in which velocity profiles were measured well into the separation region. Data were not considered where the detachment location was determined by extrapolation. Also excluded are cases where the separation is "forced" due to strong blowing or wall curvature, for example. As pointed out earlier, the subjective nature of visualization experiments is probably the cause of much of the scatter in the data of Fig. 4. Note that the data center on the point $h = 0.63$, $\Lambda = 0.42$, and scatter along the $h$-$\Lambda$ correlation of Eqs. (6) and (7).

Besides containing data from visualization experiments, Fig. 4 also contains three quantitative measurements for incipient detachment based on time-averaged fraction of forward flow $\gamma_p$. These three incipient separation locations are taken from the data of Simpson et al.,[3] Ashjaee et al.,[4] and Simpson et al.[2] They represent $\gamma_p$ values of 0.80, 0.95, and 0.80, respectively. These points are indicated by solid symbols; other points by open symbols. Note that the solid symbols lie much closer to the point $h = 0.63$, $\Lambda = 0.42$, than the older points taken by a variety of uncalibrated methods.

A correspondence between the two detachment criteria just presented and the physical picture shown in Fig. 1 can be seen by examining the experimental data presented in Fig. 5. Here, data for $\gamma_p$ vs $h$ are plotted for four different flows which follow the $h$-$\Lambda$ correlation of Eqs. (6) and (7). Three of the data sets[2-4] were measured in detaching flows, while the data of Eaton and Johnston[8] represent measurements in the reattachment region following a backward-facing step. Values of the shape parameter $h$ for the Eaton and Johnston[8] velocity profiles have been estimated with a Simpson's rule integration procedure. For this case, uncertainty bands are difficult to estimate and have been omitted purposely.

It should also be noted that the laser anemometer data of Simpson et al.[3] show large scatter for measurements taken near the test walls ($y = 2.54 \times 10^{-4}$ m). One set of these points is shown solid to indicate the scatter. For this reason, additional data are presented using the minimum values of $\gamma_p$ at each measurement location. These minimum values occur farther away from the test walls ($2.54 \times 10^{-4} \leq y \leq 2.54 \times 10^{-3}$ m), but show much less scatter than the near-wall data. Uncertainty bands are difficult to estimate and have been omitted for all the data of Simpson et al.[3]

In spite of the considerable scatter, the data of Fig. 5 indicate a direct relationship between $\gamma_p$ and $h$. The range $h = 0.63 \pm 0.06$ brackets the experimental points for $0.8 < \gamma_p < 0.95$. Accurate data sets of this type are still too few in number to be certain that $\gamma_p = f(h)$ only. Nevertheless,

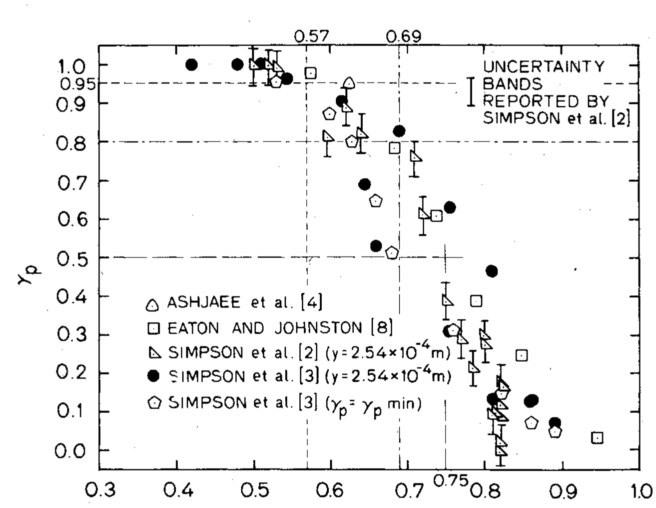


**Fig. 5 $\gamma_p$ vs $h$ for detaching and reattaching flows.**

**Table 1 Summary of detachment correlations**

| State | $\gamma_p$ | $\Lambda$ | $h$ | $H$ | $\bar{C}_f$ |
|---|---|---|---|---|---|
| Attached boundary layer | >0.95 | <0.37 | <0.55 | <2.2 | >0.0 |
| Intermittent detachment | 0.8-0.95 | 0.42 | 0.63 | 2.7 | >0.0 |
| Full detachment | ~0.5 | 0.5 | 0.75 | 4.0 | 0.0 |
| Separated region | <0.5 | >0.5 | >0.75 | >4.0 | <0.0 |

taking Fig. 4 together with Fig. 5 appears sufficient to establish the most important result. Incipient detachment can be taken as $h = 0.63 \pm 0.06$. We purposely leave the definition of incipient detachment "loose" in the sense that it implies a zone of time-averaged backflow (5-20%) that encompasses the upper "knee" of the curve (rather than a precise value). This is consistent not only with the uncertainties in available data but also with the use of the concept we envisage. We wish to correlate a zone where time-averaged backflow grows rapidly to significant values but remains well below 50%; the range 5-20% is appropriate. We can summarize these points with Table 1.

Table 1, taken with Fig. 4, not only provides a "metric" for degree of detachment, but also indicates the surprising result that both earlier experiments and earlier computational results correlate incipient rather than full detachment. Experimentally, this is probably the result of observing how far upstream the backflow of dye, particles, or tufts can be observed, and thus recording appreciable but small fractions of backflow as detachment (rather than $\gamma_p = 0.50$). Computationally, the result $1.8 < H < 2.6$ seems to have arisen from taking the point where the boundary-layer integral equations become singular as an indication of detachment. Singularities of this sort occur upstream of the location where $\bar{C}_f = 0$. For further details, see Shamroth[16] and Childs.[20] Also important here is the idea that $h = 0.63$ correlates both a significant shift in the physical behavior of the boundary layer and the start of a transition from attached to detached flow. If zonal models for the shear layers are used, it probably will be useful to re-examine the turbulence model employed whenever $h$ passes through 0.63.

For the total range of data available at present, Figs. 3-5 indicate that detachment is a function of $h$ alone. The correlation of Senoo and Nishi[10] given by Eq. (2) suggests that detachment is a direct function of the parameter $(\delta^*/W)$. We therefore need to examine this conflict.

Our opinion is that the effect of blockage in internal flow is related to detachment only through the way that it affects the freestream pressure gradient. One can see this as follows. Consider an incompressible boundary layer on the lower wall of a two-dimensional channel. Its state with respect to detachment is determined by the freestream pressure, which is, in turn, determined by the effective channel area. Assuming that the lower-wall boundary layer remains fixed, Figs. 6a and 6b show that the same effective channel area, and hence freestream pressure, can exist for two different values of $(\delta^*/W)$. Thus, channel blockage should not in itself be a factor in the detachment of the lower-wall boundary layer. We conclude that detachment is a direct function of boundary-layer state alone.

## Concept of Stall Margin

The results just presented suggest the use of either $\Lambda$ or $h$ as a "stall margin" parameter, since the correlation in Fig. 3 is roughly linear in both parameters. It is recalled that stall margin is defined as the proximity of a boundary layer to detachment. For example, let $(h_{sep} - h) = (0.63 - h)$ represent the proximity of a boundary layer to incipient detachment. The value $h_{sep} = 0.63$ is chosen, since many fluid-flow devices will show a maximum performance when the boundary layers are at incipient (but not full) detachment. Thus, the stall margin concept can be represented by the distribution of $h$ throughout the flowfield.

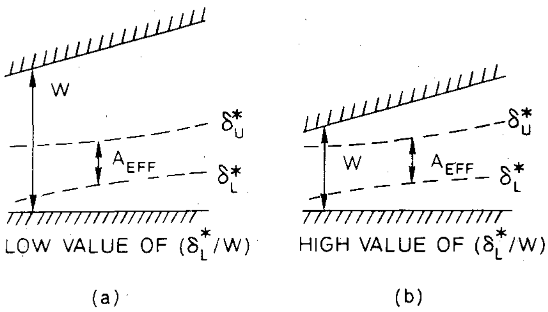


**Fig. 6 Two different values of $(\delta^*/W)$ for cases with identical lower-wall boundary layers and effective channel areas.**

In a companion paper, by Strawn and Kline,[18] this stall margin concept has been used in a design method for internal flow. Given the initial conditions, the method calculates the required flow geometry for a specified stall margin. The designer thus is able to specify how far a boundary layer will be from detachment at any given location, and to control its approach to detachment through appropriate design modifications.

## Conclusions

1) Improved one-parameter correlations for both incipient and full detachment have been established for two-dimensional turbulent boundary layers in or near equilibrium. The shape factors for each are given in Table 1. These correlations agree with a) the wall-wake law of Coles; b) the detachment criteria of Sandborn and Kline; c) the center of all older data for detachment; and d) new, more precise data on detaching flows. It is shown that earlier correlations and computations have taken incipient detachment to be full detachment.

2) Relationships have been established between the detachment correlation and the physical picture of the detachment zone, and with consequent implications for modeling and computation. This increased understanding provides a basis not only for improved prediction of detachment but also for improvements in models and numerics for zonal computational procedures.

3) The shape factor coordinates $h$-$\Lambda$ are shown to a) have powerful correlating properties for detaching and reattaching shear layers, b) provide linear (or nearly linear) correlations over a 0-1 range, and c) provide a useful measure of stall margin as a basis for indirect computation procedures.

## Acknowledgments

This paper has benefited from many discussions on details and related work within the Internal Flow and Separated Flow Research Seminars at Stanford. Contributions from the following are particularly acknowledged: J. Ashjaee, R. Childs, J. K. Eaton, J. H. Ferziger, S. Ghose, B. Gyles, J. P. Johnston, A. Lyrio, and R. Westphal.

## References

[1]Sandborn, V. A. and Kline, S. J., "Flow Models in Boundary Layer Stall Inception," *Journal of Basic Engineering, Transactions of ASME,* Vol. 83, Sept. 1961, pp. 317-327.

[2]Simpson, R. L., Strickland, J. H., and Barr, P. W., "Laser and Hot-Film Anemometer Measurement in a Separating Turbulent

Boundary Layer," Southern Methodist Univ., Tech. Rept. WT-3, 1974; see also, *Journal of Fluid Mechanics,* Vol. 79, March 1977, pp. 553-594.

[3]Simpson, F. A., Chew, Y.-T., and Shivaprasad, B. G., "Measurement of a Separating Turbulent Boundary Layer," Southern Methodist Univ., Tech. Rept. SMU-4-PU, April 1980.

[4]Ashjaee, J., Johnston, J. P., and Kline, S. J., "Subsonic Turbulent Flow in Plane Wall Diffusers: Peak Pressure Recovery and Transitory Stall," Dept. of Mech. Engrg., Stanford Univ., Stanford, Calif., Rept. PD-21, July 1980; also, *Journal of Fluids Engineering, Transactions of ASME,* Vol. 102, Sept. 1980, pp. 275-282.

[5]Eaton, J. K., Jeans, A. H., Ashjaee, J., and Johnston, J. P., "A Wall-Flow Direction Probe for Use in Separating and Reattaching Flows," *Journal of Fluids Engineering, Transactions of ASME,* Vol. 101, Sept. 1979, pp. 364-366.

[6]Schraub, F. A. and Kline, S. J., "A Study of the Structure of the Turbulent Boundary Layer With and Without Longitudinal Pressure Gradient," Dept. of Mech. Engrg., Stanford Univ., Stanford, Calif., Rept. MD-12, March 1965.

[7]Kline, S. J., Reynolds, W. C., Schraub, F. A., and Runstadler, P. W., "Structure of the Turbulent Boundary Layer on a Smooth Wall," *Journal of Fluid Mechanics,* Vol. 30, Dec. 1967, pp. 741-773.

[8]Eaton, J. K. and Johnston, J. P., "Turbulent Flow Reattachment: An Experimental Study of the Flow and Structure Behind a Backward-Facing Step," Dept. of Mech. Engrg., Stanford Univ., Stanford, Calif., Rept. MD-39, June 1980.

[9]Cebeci, T. and Bradshaw, P., *Momentum Transfer in Boundary Layers,* McGraw Hill Book Co., New York, 1977, p. 194.

[10]Senoo, Y. and Nishi, M., "Prediction of Flow Separation in a Diffuser by a Boundary Layer Calculation," *Journal of Fluids Engineering, Transactions of ASME,* Vol. 99, 1975, pp. 379-389.

[11]Coles, D., "The Law of the Wake in the Turbulent Boundary Layer," *Journal of Fluid Mechanics,* Vol. 1, July 1956, pp. 191-226.

[12]Coles, D. E. and Hirst, E. A., ed., *Computation of Turbulent Boundary Layers—1968,* AFOSR-IFP-Stanford Conference, Vol. II, Dept. of Mech. Engrg., Stanford Univ., Stanford, Calif., 1969.

[13]Ghose, S. and Kline, S. J., "Prediction of Transitory Stall in Two-Dimensional Diffusers," Dept. of Mech. Engrg., Stanford Univ., Stanford, Calif., Rept. MD-36, Dec. 1976; see also, *Journal of Fluids Engineering, Transactions of ASME,* Vol. 100, Dec. 1978, pp. 419-426.

[14]Kuhn, G. D. and Nielsen, J. N., "An Analytical Method for Calculating Turbulent Separated Flows Due to Adverse Pressure Gradients," Project SQUID, TR NEAR-1-PU, Oct. 1971.

[15]Bardina, J., Lyrio, A. A., Kline, S. J., Ferziger, J. H., and Johnston, J. P., "A Prediction Method for Planar Diffuser Flows," *Journal of Fluids Engineering, Transactions of ASME,* Vol. 103, June 1981, pp. 315-321.

[16]Shamroth, S. J., "On Integral Methods for Predicting Shear Layer Behavior," *Journal of Applied Mechanics, Transactions of ASME,* Vol. 36, Dec. 1969, pp. 673-681.

[17]Kim, J., Kline, S. J., and Johnston, J. P., "Investigation of Separation and Reattachment of a Turbulent Shear Layer: Flow over a Backward-Facing Step," Thermosciences Div., Dept. of Mech. Engrg., Stanford Univ., Stanford, Calif., Rept. MD-37, April 1978.

[18]Strawn, R. C. and Kline, S. J., "A Stall Margin Design Method for Planar and Axisymmetric Diffusers," presented at ASME Winter Annual Meeting, Nov. 14-19, 1982; to be published in *Journal of Fluids Engineering, Transactions of ASME.*

[19]Sandborn, V. A., "An Equation for the Mean Velocity Distribution of Boundary Layers," NACA Memo. 2-5-59E, 1958.

[20]Childs, R., Ferziger, J. H., and Kline, S. J., "A Computational Method for Subsonic Compressible Flow in Diffusers," Dept. of Mech. Engrg., Stanford Univ., Stanford, Calif., Rept. PD-24, Oct. 1981.

[21]Gillis, J. C., Johnston, J. P., Kays, W. M., and Moffat, R. J., "Turbulent Boundary Layer on a Convex, Curved Surface," Dept. of Mech. Engrg., Stanford Univ., Stanford, Calif., Rept. HMT-31, Sept. 1980.

[22]Schubauer, G. and Klebanoff, P., "Investigation of Separation of the Turbulent Boundary Layer," NACA TN 2133, 1950; also, NACA TR 1030, 1951.

[23]Newman, B. G., "Some Contributions to the Study of the Turbulent Boundary Layer Near Separation," Dept. of Supply, Aeronautical Research Consultative Committee, Australia, Rept. ACA-53, March 1951.

[24]Strickland, J. H. and Simpson, R. L., "The Separating Turbulent Boundary Layer: An Experimental Study of an Airfoil-Type Flow," Southern Methodist Univ., Tech. Rept. WT-2, Aug. 1973.

[25]Stratford, B. S., "An Experimental Flow with Zero Skin Friction Throughout Its Region of Pressure Rise," *Journal of Fluid Mechanics,* Vol. 5, July 1958, pp. 17-35.

[26]Doenhoff, A. E. and Tetervin, N., "Determination of General Relations for the Behavior of Turbulent Boundary Layers," NACA 772, 1943.

[27]Murphy, J. S., "The Separation of Axially Symmetric Turbulent Boundary Layers," Part I, Douglas Aircraft Co., Rept. ES 17513, 1955.

[28]Hewson, C. T., "Growth and Separation of a Turbulent Boundary Layer," ASME Symposium on Stall, 1958.

[29]Fraser, H. R., "The Turbulent Boundary Layer in a Conical Diffuser," *Journal of Hydraulic Division, Proceedings of the ASCE,* Vol. 84, No. H43, 1958, p. 1684.

[30]Moses, H. L., "The Behavior of Turbulent Boundary Layers in Adverse Pressure Gradients," MIT Gas Turbine Lab., Rept. No. 73, 1964.

[31]Sandborn, V. A., "Preliminary Experimental Investigation of Low-Speed Turbulent Boundary Layers in Adverse Pressure Gradients," NACA TN 3031, 1953.